Strain based finite fracture mechanics for fatigue life prediction of additively manufactured samples

Int J Fract (2025) 249:44
https://doi.org/10.1007/s10704-025-00855-1

RESEARCH

Strain based finite fracture mechanics for fatigue life prediction of additively manufactured samples

A. M. Mirzaei · A. H. Mirzaei · A. Sapora · P. Cornetti

Received: 30 December 2024 / Accepted: 9 May 2025 / Published online: 12 June 2025

Abstract A novel failure criterion, named Strain-based Finite Fracture Mechanics, is proposed to predict the fatigue life of additively manufactured notched components under uniaxial loading conditions. The model relies on the simultaneous fulfillment of two conditions: a non-local strain requirement and the discrete energy balance. The inputs of the model are strain and the stress intensity factor at failure, which depend on the number of cycles according to power law equations. The inputs can be obtained based on strain-life and stress intensity factor-life data from plain and notched specimens. The present approach is comprehensively validated against experimental datasets on additively manufactured samples from the literature for different materials, raster angles, notch geometries and loading conditions. Predictions by other approaches, such as Finite Fracture Mechanics (in its original stress formulation) and the Theory of Critical Distances, are also considered, for the sake of completeness. Results show that, in general, the proposed strain-based model is more accurate and provides consistently precise predictions across different cases.

Keywords Coupled criterion · Additive manufactured samples · Notched samples · Strain based criterion · Energy based criterion

A. M. Mirzaei (✉) · A. Sapora · P. Cornetti
Department of Structural, Geotechnical and Building Engineering, Politecnico di Torino, Corso Duca Degli Abruzzi 24, 10129 Turin, Italy
e-mail: amir.mirzaei@polito.it

A. M. Mirzaei
Faculty of Engineering and Applied Science, Cranfield University, Cranfield MK43 0AL, UK

A. H. Mirzaei
Department of Mechanical and Industrial Engineering, Norwegian University of Science and Technology, Trondheim, Norway

Nomenclatures

A	Length of a crack originating from the notch root
a_e, b_e	Basquin's parameters for ε_f
a_k, b_k	Basquin's parameters for K_{If}
E	Elastic modulus
g_e	Geometrical function for the normal strain field
g_k	Geometrical function for the stress intensity factor (SIF)
K_I	Mode I SIF
K_{Ic}	Plane strain fracture toughness
K_{If}	SIF at failure
L	Crack advancement for the FFM formulation in the fatigue life regime
l_c	Critical distance for the MTSN model in the static regime
l_f	Critical crack advancement for the FFM formulation in the fatigue life regime
N	Number of cycles

N_f	Number of cycles to failure
R	Loading ratio
r	Notch radius
α	Notch opening angle
ε_y	Normal strain component
v	Poisson's ratio
σ_a	Nominal (gross-section) stress amplitude
σ_c	Material characteristic strength
σ_x, σ_y	Stress components in the Cartesian coordinate system (x, y)
θ_p	Principal printing direction

1 Introduction

Additive manufacturing is considered a revolutionary manufacturing process that offers many advantages compared to traditional manufacturing methods, such as greater design flexibility, reduced material waste, faster production, and cost efficiency. These advantages have made additive manufacturing an increasingly popular option in various industrial sectors, including aerospace and healthcare (Kholgh Eshkalak et al. 2020; Song et al. 2020). The progress in this method is transforming the way we design, create, and produce mechanical components (Lewandowski and Seifi 2016; Ezeh and Susmel 2019; Blakey-Milner et al. 2021). However, in order to fulfill the design requirements and account for working conditions—especially in the case of additively manufactured (AM) components where defects may arise during the manufacturing process, it becomes crucial to take into account the potential presence of cracks, holes, or notches in the AM specimens (Gebhardt et al. 2022; Meyer et al. 2022). These defects act as stress concentrators and can impair the strength and service life of structures (Salvati et al. 2020; Mirzaei et al. 2021a). Therefore, it is crucial to examine the behavior of AM samples weakened by such flaws under the most common failure mechanism in real structures, which is fatigue loading.

One successful approach for assessing the failure of notched components is the Theory of Critical Distances (TCD). This approach, dating back to Whitney & Nuismer (1974) and refined by Taylor (1999) and Susmel (2009), rests on an internal length scale: failure occurs when the stress component at or along the critical distance reaches its critical value, typically the ultimate strength of the material for static brittle failure. The TCD approach has been widely accepted and applied in the design and analysis of structures with notches or other stress concentration features under quasi-static loading conditions (Susmel and Taylor 2008a, b; Ayatollahi and Torabi 2010; Schmidt et al. 2020), including inhomogeneous materials like additively manufactured samples (Marsavina et al. 2023). Susmel and Taylor (2007) further extended the TCD approach to estimate the fatigue life of notched components in the medium-cycle fatigue regime, specifically within 10^3–10^6 cycles. The extension was based on the idea that the critical distance varies as a power law with the number of cycles to failure in the medium/high cycle fatigue regime. The approach has been applied to a number of fatigue problems related to isotropic materials under different loading conditions such as uniaxial (Zhu et al. 2020), torsional (Susmel and Taylor 2013), multiaxial (Susmel and Taylor 2008c; Branco et al. 2021), variable amplitude (Susmel and Taylor 2011, 2015), and elasto-plastic materials in the low- and medium-cycle fatigue regimes (Susmel and Taylor 2010). More recently, TCD has also been applied to additively manufactured samples (Benedetti and Santus 2019; Ezeh and Susmel 2020; Molaei and Fatemi 2021; Molaei et al. 2022). Notably, in (Ezeh and Susmel 2020), the Authors argued that the overall fatigue strength of additively manufactured Polylactic Acid (PLA) may not be significantly influenced by the raster angle in the presence of stress concentration phenomena.

Considering failure analysis of structures, it has been demonstrated that some materials exhibit strain-controlled failure, e.g. bones (Nalla et al. 2003). Moreover, strain-based criteria prove to be more accurate in predicting failure for materials that exhibit more significant plastic deformation (Jia and Bai 2016; Mirzaei and Shokrieh 2024). Therefore, having a reliable strain-based failure criterion can be helpful. In structural analysis using the TCD approach, it is commonly assumed that the stress component normal to the potential crack at fracture onset is the critical parameter for predicting failure. Starting from the widely recognized criterion by Saint Venant (Timoshenko 1983) known as the maximum normal strain criterion, Chang (1981) proposed a non-local version of this criterion to deal with mixed mode cracked geometries, i.e. assuming failure occurs when

the maximum strain at a given (critical) distance from the notch tip reaches a threshold value, and named it Maximum Tangential (hoop) Strain (MTSN) criterion. Next, the MTSN criterion was analytically developed by Mirsayar, who took the effect of the first non-singular term into account and utilized it to estimate the failure and crack initiation angle for specimens made of PMMA (Mirsayar 2015), rock (Mirsayar et al. 2018), and even orthotropic composites (Mirsayar 2022) under quasi-static loading conditions. The MTSN method was also exploited for failure estimation in different problems, such as human bones (Nalla et al. 2003), size effect (Aghabeigi et al. 2024), mixed mode I/III (Bidadi et al. 2022), and wing-crack initiation under uniaxial compression (Zhu et al. 2021). Considering fatigue loading, Burke-Veliz et al. (2010) simulated the crack propagation shielding and deflection in plain bearings under large-scale yielding during cyclic loading. Finally, in (Shi et al. 2020), the MTSN criterion was utilized to investigate the fatigue life of Al-steel resistance spot welds.

Whilst the critical distance in the TCD approaches is a material property, in the Finite Fracture Mechanics (FFM) approach, originally proposed by Leguillon (2002) and Cornetti et al. (2006), the finite crack advance is not known a priori, being a function of the geometry and loading conditions beyond the material properties. According to FFM, the failure load and the crack advancement are obtained by solving a system of two equations, representing a stress and an energy condition for the crack onset. It is worth noting that the FFM is also known as the Coupled Criterion, particularly regarding Leguillon's formulation (2002), emphasizing that both energy and stress conditions must be satisfied for crack propagation to occur. The model has been successfully employed for various structures and materials, including notched specimens under different loading conditions such as mode I (Carpinteri et al. 2008, 2011), mode II (Sapora et al. 2014; Campagnolo et al. 2016), and mixed mode (Yosibash et al. 2006; Priel et al. 2008; Cornetti et al. 2013; Doitrand et al. 2021) failures. Moreover, the FFM approach has been applied to examine the failure of notched composites (Camanho et al. 2012) and to perform debonding analyses (Carpinteri et al. 2009; Mirzaei et al. 2021b). Remarkably, by coupling the Hencky strain tensor and the discrete energy balance, Rosendahl et al. (2019) studied the mixed-mode crack nucleation in structural glazing silicone sealants under static loading conditions. Recently, Mirzaei et al. (2023) extended the Finite Fracture Mechanics model to the finite fatigue life regime. They assumed that the critical parameters of the model, namely cyclic strength and stress intensity factor at failure, depend on the number of cycles following power law equations.

Considering the need for a reliable strain-based failure criterion, the FFM model we propose in the next section combines the maximum normal strain and discrete energy balance to predict the failure of notched specimens. Under cyclic uniaxial loading conditions, the model will be validated using a comprehensive range of experimental data on AM samples from the literature and compared with (stress) FFM and TCD approaches.

The plan of the paper is as follows. In Sect. 2, we briefly review the TCD and FFM failure models for monotonic and fatigue loading, and then present the novel, strain-based FFM model. In Sect. 3, we introduce the experimental data, along with their specifications, that we aim to interpret. In Sect. 4, we present the results and analyze their performance with respect to the different experimental programs considered. Finally, conclusions are provided in Sect. 5.

2 Modeling approach

In this section, a concise introduction to MTSN and FFM in their original formulations is provided. Subsequently, the proposed strain-based Finite Fracture Mechanics (EFFM) model is introduced for finite fatigue life assessment.

Before starting, it is important to highlight some of the advantages of a strain-based criterion over a stress-based one. Firstly, strain-based criteria are often more reliable in predicting failure in quasi-brittle materials and in materials that exhibit significant plastic deformation, even when these deformations occur within the small-scale yielding regime (Wu and Cervera 2016). Secondly, such criteria can effectively distinguish between plane stress and plane strain conditions, which is critical for accurate failure predictions. Thirdly, strain measurement is much more straightforward than stress measurement, as it directly relates to observable deformations and displacements. This allows for the convenient application of in-situ techniques like digital image correlation or

photoelasticity to obtain strain distribution. Specifically for fatigue loading, industries prefer strain-based fatigue life analysis because it provides more accurate and reliable predictions by directly using experimentally measured strain, which better represents material behavior under complex or localized loading conditions (Zhao et al. 1998). Fourthly, determining the elastic modulus, particularly in inhomogeneous materials such as bone, can be complex due to material variability, making stress evaluation from experimental data a challenging task (Dong et al. 2010; Wang et al. 2023). Fifthly, since damage is often a strain-controlled phenomenon in deformation-dominated materials, strain-based criteria are generally more suitable for cases where damage is the primary failure mechanism (Challamel et al. 2005). Finally, strain-based criteria often better capture the anisotropic behavior of materials, particularly in composites and other directionally dependent systems (Zywicz 1999).

2.1 MTSN model for quasi-static loading

The MTSN criterion in mode I loading, as proposed by Chang (1981), postulates that failure occurs when the maximum normal strain, ε_y, reaches its critical value, $\varepsilon_c = \sigma_c/E$, at a critical distance, l_c, from the notch root:

$$\varepsilon_y(l_c) = \varepsilon_c \tag{1}$$

As such, the MTSN falls within the TCD approach. The normal strain (under plane stress conditions) and the critical distance can be obtained as:

$$\varepsilon_y = \frac{1}{E}\left(\sigma_y - \nu\,\sigma_x\right) \tag{2}$$

$$l_c = \frac{1}{2\pi}\left[\frac{K_{Ic}(1-\nu)}{\sigma_c}\right]^2 \tag{3}$$

where ν the Poisson's ratio, σ_x and σ_y are the stress components in the Cartesian coordinate system (before crack nucleation) and K_{Ic} is plane strain fracture toughness. Interestingly, by setting $\nu = 0$ in Eq. (1), the point method of (stress-based) TCD can be recovered.

It is worth noting that, although Chang (1981) originally proposed the MTSN criterion based on the pointwise method, the criterion can be straightforwardly rewritten based on the averaged strain along the bisector line as follows:

$$\frac{1}{l_c}\int_0^{l_c} \varepsilon_y(x)\,\mathrm{d}x = \varepsilon_c \tag{4}$$

with:

$$l_c = \frac{2}{\pi}\left[\frac{K_{Ic}(1-\nu)}{\sigma_c}\right]^2 \tag{5}$$

2.2 FFM model for fatigue loading

It is worthwhile to emphasize that the present analysis focuses on the medium/high-cycle fatigue regime, assuming that the dominant stage of crack growth during fatigue life is stage II, where the crack establishes perpendicular to the loading direction. Consequently, in the analyses, only mode I relations are considered. Additionally, it is assumed that the effect of plastic zone size can be neglected, allowing for the determination of the strain field and energy release rate ahead of the notch tip using linear elastic mechanics (see (Mirone 2004) for a deeper insight).

The FFM approach states that failure occurs when both stress and energy conditions are simultaneously satisfied, leading to the formation of a crack of length l (Leguillon 2002; Cornetti et al. 2006). The FFM criterion was extended to the finite fatigue life regime by Mirzaei et al. (2023), based on the idea that the input material properties, i.e. critical strength and Stress Intensity Factor (SIF), evolve as functions of the number of cycles N, following the SN data of both plain and notched (cracked) samples. Focusing on fatigue loading, the FFM approach for an arbitrary

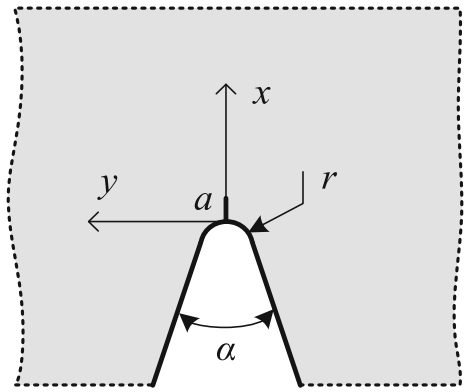

Fig. 1 Schematic view of a notch geometry and Cartesian coordinate system located at its tip

notched geometry, as shown in Fig. 1, can be represented by Eq. (6):

$$\begin{cases} \dfrac{1}{l}\displaystyle\int_0^l \sigma_y(x)\,dx = \sigma_c(N) = a_s\,N^{-b_s} \\ \dfrac{1}{l}\displaystyle\int_0^l K_I^2(a)\,da = K_{Ic}^2(N) = \left(a_k\,N^{-b_k}\right)^2 \end{cases} \tag{6}$$

The first equation addresses the stress requirement, stating that at failure, the normal stress σ_y, averaged over the discrete crack advance, l, must meet the cyclic strength, $\sigma_c(N)$. The second equation involves the discrete energy balance, which requires that the strain energy release for a finite crack extension, l, equals the cyclic fracture energy $G_c(N)$ times l. Note that in Eq. (6), the energy condition has been rewritten in terms of SIF by using Irwin's relationship. It is worth emphasizing that Eq. (6) is a system of two equations in two unknowns, whose solutions are the critical crack advance l_f and number of cycles to failure N_f. Both solutions are clearly dependent on material properties and geometry. It can be seen that power law equations are considered to capture the dependency of material parameters on the number of cycles, N, which will be elaborated on in Eqs. (7) and (8).

2.3 EFFM model for fatigue loading

By coupling the strain and strain energy release criteria in the framework of FFM (replacing the average stress requirement in Eq. (6) with the strain criterion Eq. (4)), the EFFM model for predicting the fatigue life of notched components is achieved.

In order to develop the model for finite life estimation, a couple of material properties are now introduced: ε_f and K_{If}, here simply termed cyclic strain and cyclic SIF at failure. It is assumed that ε_f and K_{If}, which are lower than their static counterparts ε_c and K_{Ic}, depend on the number of cycles N, and their variation in the medium/high cycle fatigue regime can be captured by means of power-law relations (Susmel 2009; Ciavarella et al. 2017), namely:

$$\varepsilon_f = \varepsilon_f(N) = a_e\,N^{-b_e} \tag{7}$$

$$K_{If} = K_{If}(N) = a_k\,N^{-b_k} \tag{8}$$

where a_e, b_e and a_k, b_k are positive coefficients, which are functions of both material properties and loading conditions. Equations (7) and (8) are in the form of Basquin's equations (Basquin 1910). A more detailed explanation of the determination of the coefficients is provided in Sect. 3.

Then, by means of Eqs. (7) and (8), EFFM can be cast in the following form:

$$\begin{cases} \dfrac{1}{l}\displaystyle\int_0^l \varepsilon_y(x)\,dx = a_e\,N^{-b_e} \\ \dfrac{1}{l}\displaystyle\int_0^l K_I^2(a)\,da = a_k^2\,N^{-2b_k} \end{cases} \tag{9}$$

Note that the latter equation coincides with the second one in Eq. (6). Similar to Eq. (6), Eq. (9) represents a system of two equations in two unknowns: the number of cycles to failure N_f, and the crack advancement l_f. From a physical perspective, Eq. (9) implies that failure is energy-driven, but a strain level that is high enough must be present to trigger crack propagation. Note that l_f values for EFFM and FFM criteria are clearly different.

Using linear elastic relationships, the maximum normal strain amplitude can be expressed as $\varepsilon_y(x) = (\sigma_a/E)\,g_e(x,v)$ where σ_a is the nominal (gross-section) stress amplitude and g_e is a proper function of the spatial coordinate x and Poisson's ratio v. Analogously, the SIF amplitude can also be defined as a product of the nominal (gross-section) stress amplitude and a geometrical function, $K_I(a) = \sigma_a\,g_k(a)$. Note that the functions $g_e(x,v)$ and $g_k(a)$ are fixed for a given geometry and material. Finally, Eq. (9) can be rewritten as:

$$\begin{cases} N = l^{1/b_e}\left[\dfrac{\sigma_a}{E\,a_e}\displaystyle\int_0^l g_e(x,v)\,dx\right]^{-1/b_e} \\ N = \sqrt{l^{1/b_k}\left[\left(\dfrac{\sigma_a}{a_k}\right)^2\displaystyle\int_0^l g_k^2(a)\,da\right]^{-1/b_k}} \end{cases} \tag{10}$$

Equation (10) can be solved using a procedure analogous to Eq. (6). It is clear that the proposed model is simple and easy to use, as it does not require sophisticated coding. Moreover, it has a sound physical meaning without any fitting parameters.

3 Experimental data for EFFM validation and parameters calibration procedure

In this section, we briefly present the experimental datasets used to verify the EFFM model. This includes the material properties, geometrical specifications, and loading conditions. The procedure for calibrating the required parameters of the proposed model under fatigue loading is also elaborated.

To verify the accuracy of the proposed model for finite fatigue life estimation, five experimental datasets are considered. The first and second datasets involve PLA samples with three different manufacturing angles ($\theta_p = 0°, 30°, 45°$) (Ezeh and Susmel 2020), which were tested under two different load ratios ($R = -1$ and 0), while the third dataset comprises Inconel 718 specimens (Solberg and Berto 2019) tested under a load ratio of $R = 0$. The fourth and fifth datasets are related to samples made of Ti6Al4V (Zamzami et al. 2020), which again were tested under load ratios of $R = -1$ and 0.1. The geometry of the samples used in all datasets is shown schematically in Fig. 2 with their respective geometrical parameters. Table 1 summarizes the material properties, geometrical specifications, and fatigue test conditions of these datasets. For the first and second datasets, θ_p is the angle between the sample's longitudinal axis and its principal manufacturing direction (see Fig. 2). In these datasets, despite varying manufacturing angles, the effect of filament orientation on mechanical properties is deemed negligible. For a more detailed analysis, refer to Ezeh and Susmel (2019). Note that, due to the relatively small thickness of the samples, as mentioned in Table 1, the specimens are modeled under plane stress conditions, and the calculations are based on this assumption.

In order to implement the EFFM approach for cyclic loading, it is necessary to determine the parameters a_e and b_e (Eq. 7) and a_k and b_k (Eq. 8), which describe the variation of the cyclic strain and stress intensity factor at failure with respect to the number of cycles, respectively. Whereas a_e and b_e are determined using the strain-life data of a plain specimen, a_k and b_k can be obtained using SIF-life data of a cracked sample (Carpinteri and Paggi 2009; Castillo et al. 2014; Sanaei and Fatemi 2020; Miarka et al. 2022). Strain-life can be calculated straightforwardly using SN data and E, while the SIF-life requires a simple calculation of the SIF for the cracked geometry under the considered loading amplitude.

Based on the information provided above, the simplest approach would be to exploit the data referring to the two extreme cases of low cycle and high cycle fatigue (fatigue limit, if it exists). A second approach is to employ all the data within the range of finite fatigue life and to perform an overall best-fitting procedure for data with 50% survival probability. Clearly, the second approach may result in higher accuracy, due to the use of a larger dataset and reducing the typically high scatter of fatigue experimental data. Besides, obtaining data related to the two extremes can be challenging, especially in case of static loading (low cycle fatigue).

Observe that, in the case that a cracked specimen is not available, an inverse calibration of Eq. (8) can be performed using the data related to a notched sample and Eq. (10): knowing the fatigue life and the applied stress amplitude of the notched sample, the former

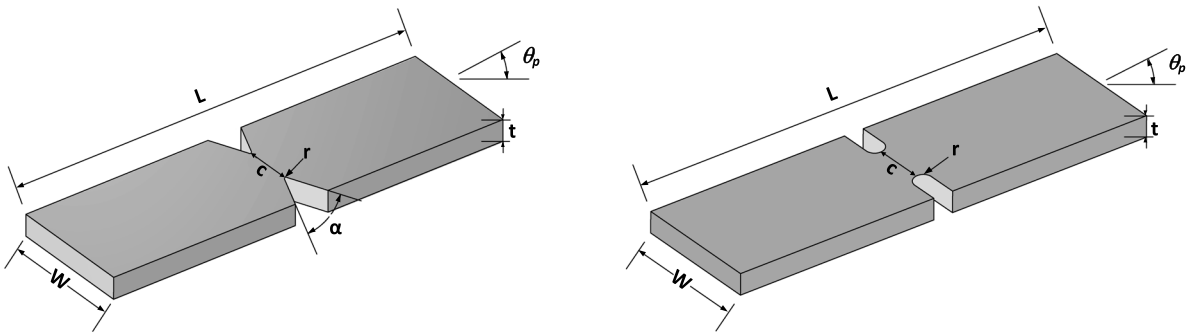

Fig. 2 Geometries under investigation: **a** double symmetric V-notched sample; **b** double symmetric U-notched sample

Table 1 Specification of the employed experimental data for fatigue life prediction

Set No	Material properties			Geometrical specifications				Loading ratio
	Name	E (MPa)	v	t (mm)	W (mm)	L (mm)	Stress raiser (lengths in mm)	R
1&2	PLA	3476	0.33	3	25	–	plain specimen: $c = 6$	− 1 and 0
						86	U-notch: $c = 6$, $r = 3$	
						82	U-notch: $c = 6$, $r = 1$	
						86	V-notch: $\alpha = 35°$, $c = 6$, $r = 0.15$	
3	Inconel 718	200 000	0.29	5	15	80	plain specimen: $c = 7$	0
							semi-circular notch: $c = 5$, $r = 5$	
							V-notch: $\alpha = 90°$, $c = 5$, $r = 1$	
							V-notch: $\alpha = 90°$, $c = 5$, $r = 0.1$	
4&5	Ti6Al4V	110 000	0.33	2.7	12.1	80*	plain specimen: $c = 4.7$	− 1 and 0.1
							U-notch: $c = 5.8$, $r = 0.7$	
							U-notch: $c = 6$, $r = 1.5$	
							V-notch: $\alpha = 35°$, $c = 4.7$, $r = 0.4$	

*The length of samples was not presented in the paper; we assume it long enough to eliminate its effect

equation in the EFFM system provides $l_f(N)$ and the latter one yields $K_{If}(N)$. Note that it is advisable to use the sharpest notch geometry data to calibrate $K_{If}(N)$, in order to achieve the highest accuracy (Taylor et al. 2000; Susmel and Taylor 2007; Ciavarella et al. 2017).

In this paper, we adopt the second approach of employing all the data within the finite life range. Since a cracked geometry was not tested in the experimental campaign (see Table 1), inverse calibration using the V-notched samples with the smallest notch tip radii is employed to obtain a_k and b_k. The calculated parameters for all datasets are presented in Table 2.

It is worth mentioning that the asymptotic stress solution proposed by Mirzaei et al. (2021a) was utilized to calculate the maximum normal strain along the notch bisector line, i.e., the function $g_e(x,v)$. This solution allowed us to determine the strain field ahead of the notch tip, even at large distances by considering the effect of higher order terms (Mirzaei et al. 2019, 2020) (the first three terms were considered in this study). Additionally, Finite Element Analyses were conducted for each geometry in order to compute K_I as a function of crack length (i.e., the function $g_k(a)$) and to validate the analytical expressions used for the strain field. The samples were meshed using 8-node

Table 2 Calculated parameters of the EFFM model for the studied cases

Material	R	Equation (7): $\varepsilon_f(N) = a_e N^{-b_e}$	Equation (8): $K_{If}(N) = a_k N^{-b_k}$ [MPa $\sqrt{m}$]
PLA	0	$a_e = 0.014$	$a_k = 15.20$
		$b_e = 0.161$	$b_k = 0.276$
	− 1	$a_e = 0.042$	$a_k = 7.600$
		$b_e = 0.232$	$b_k = 0.208$
Inconel 718	0	$a_e = 0.651$	$a_k = 532.0$
		$b_e = 0.272$	$b_k = 0.317$
Ti6Al4V	0.1	$a_e = 0.042$	$a_k = 48.30$
		$b_e = 0.303$	$b_k = 0.199$
	− 1	$a_e = 0.072$	$a_k = 185.0$
		$b_e = 0.357$	$b_k = 0.291$

biquadratic elements, and a mesh convergence analysis was performed to ensure that the numerical results were not affected by mesh size.

4 Results and discussion

In this section, we compare EFFM predictions with the experimental datasets presented earlier and with the theoretical approaches mentioned previously, specifically the stress-based FFM and TCD approaches, to evaluate the fatigue life of AM specimens. To the best of the authors' knowledge, the MTSN model is not specifically designed for predicting finite fatigue behavior in materials. Consequently, the comparison of EFFM results is limited to other well-established criteria, such as FFM and TCD. It is worth emphasizing that comparing the results with the Line Method (LM, (Taylor 1999)), which is a part of the TCD framework, is more appropriate because it also involves stress averaging over the critical distance, similar to how EFFM utilizes the strain field. However, LM cannot be applied to all datasets because, in some cases, the critical distance exceeds the net width of the PLA samples (Ezeh and Susmel 2020), illustrating one of the primary limitations of the TCD method.

For the sake of brevity, the details of each model are not fully discussed for fatigue tests. Nevertheless, further information about TCD approach and its necessary parameters are found in (Ezeh and Susmel 2020) for samples made of PLA, and in (Zamzami et al. 2020) regarding samples made of Ti6Al4V. Additionally, reference (Mirzaei et al. 2023) provides comprehensive information on the FFM model for finite fatigue life analyses.

Before presenting the results, it is advisable to introduce two indicators that are used to quantify and visualize the accuracy of the EFFM, FFM (Mirzaei et al. 2023), and TCD (Susmel and Taylor 2007) models against experimental data. First, we employed the Symmetric Mean Absolute Percentage Error (SMAPE), which ranges from 0 to 100%, with lower SMAPE values indicating more precise predictions. The formula we utilized for calculating the SMAPE is:

$$\text{SMAPE} = \frac{100}{n}\sum_{1}^{n}\frac{\left|N_{\text{f,exp}} - N_f\right|}{\left(N_{\text{f,exp}} + N_f\right)} \tag{11}$$

where n is the total number of tests.

Second, following (Ince and Glinka 2011; Zhu et al. 2017), we evaluated the logarithmic error per each data point, defined as:

$$\text{Error} = \text{Log}\left(\frac{N_{\text{f,exp}}}{N_{\text{f}}}\right) = \text{Log}\,N_{\text{f,exp}} - \text{Log}\,N_{\text{f}} \tag{12}$$

Considering the logarithmic error as a statistical variable, we computed its probability density function (PDF). The PDFs shown in the figures are empirical estimates derived using the SmoothKernelDistribution function in Mathematica, which applies kernel density estimation to the logarithmic residuals (Log10[exactData/predictedData]), rather than assuming a specific parametric form such as a normal or Weibull distribution. According to Eq. (12), positive errors correlate to conservative predictions and vice-versa.

For the specimens made of PLA (Zhu et al. 2017), Figs. 3 and 4 present the experimental number of cycles to failure and the corresponding theoretical predictions using the EFFM, FFM, and TCD models for the load ratios of 0 and -1, respectively. It should be noted that the horizontal axis represents the estimated life, while the vertical axis corresponds to the experimental data. The solid line (45° line) indicates exact predictions, while the triangular region above/below the solid line illustrates the conservative/overestimating region. The dashed blue lines represent 1/3 and 3 scatter bands, and the dot-dashed gray lines illustrate 1/5 and 5 scatter bands.

The results presented in Figs. 3 and 4 demonstrate that the fatigue lifetime predicted by the EFFM model is in good agreement with the experimental data provided in (Ezeh and Susmel 2020). Comparing EFFM to FFM, the proposed model provides higher accuracy for $R = 0$ (SMAPE: 21.9% versus 33.2%) and marginally improved accuracy for $R = -1$ (SMAPE: 20.7% versus 21.4%). Furthermore, the accuracy of the predicted results by the EFFM model is higher compared to that of the TCD method. The SMAPE values for the $R = 0$ case (Fig. 3) are 21.9% and 50.3% for the EFFM model and TCD model, respectively, indicating a significant improvement. A smaller yet significant improvement is achieved for $R = -1$ (Fig. 4), with SMAPE values of 20.7% and 25.2% for the EFFM model and TCD model, respectively. An interesting finding is that the same set of data was employed in (Mirzaei 2024) to validate a

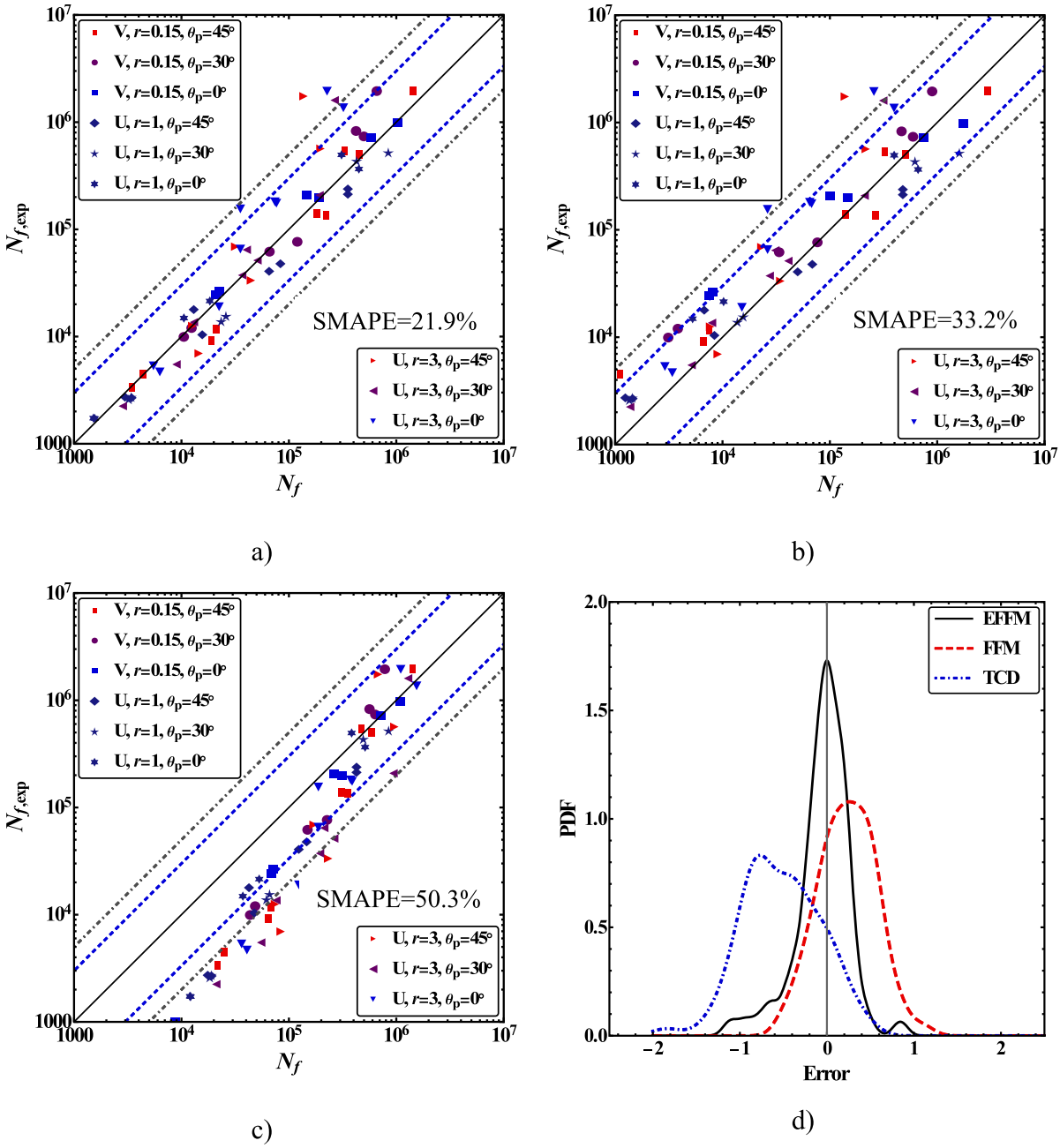

Fig. 3 Number of cycles to failure for different notch geometries and manufacturing angles made of PLA under fatigue loading with loading ratio $R = 0$, experimental data (Ezeh and Susmel 2020) vs. estimations by **a** EFFM, **b** FFM and **c** TCD methods. **d** Shows the PDF of the logarithmic error in the prediction of fatigue lifetime using EFFM, FFM, and TCD methods

novel machine learning-based model for estimating the fatigue life of notched components, and the results show that using the strain field as input yields slightly more accurate predictions than using the stress field.

Additionally, when comparing the logarithmic error PDF, it becomes evident that the EFFM model performs better in predicting the fatigue life of the specimens. Figures 3 and 4 illustrate that the error

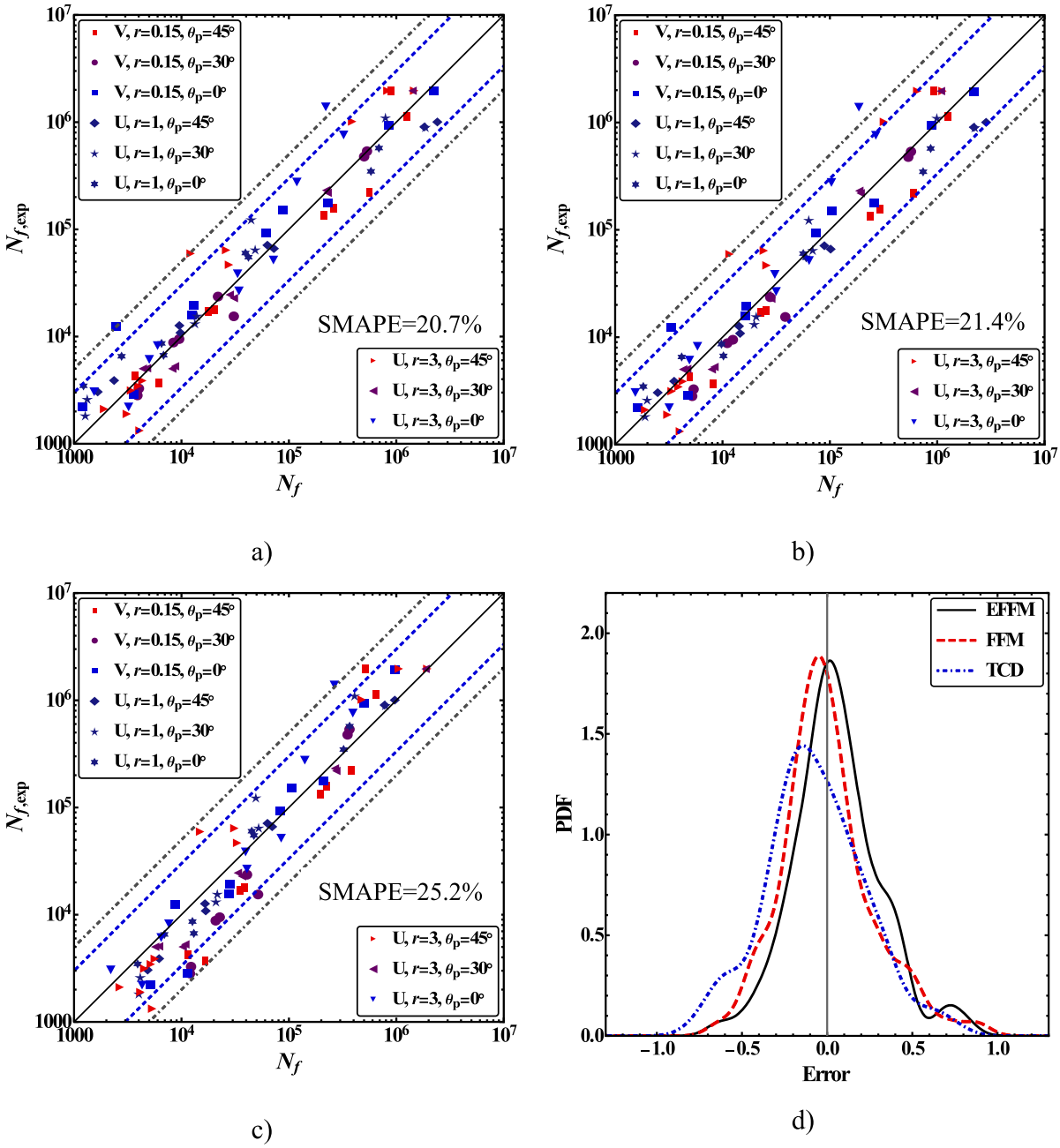

Fig. 4 Number of cycles to failure for different notch geometries and manufacturing angles made of PLA under fatigue loading with loading ratio $R = -1$, experimental data (Ezeh and Susmel 2020) vs. estimations by **a** EFFM, **b** FFM and **c** TCD methods. **d** Shows the PDF of the logarithmic error in the prediction of fatigue lifetime using EFFM, FFM and TCD methods

distribution of the EFFM model is more compact and exhibits smaller variance. This indicates that the results predicted by the EFFM model are more consistent and reliable. In contrast, the TCD approach tends to yield nonconservative fatigue life estimations, particularly for the case with $R = 0$.

Regarding the dataset consisting of specimens made of Inconel 718 (Solberg and Berto 2019),

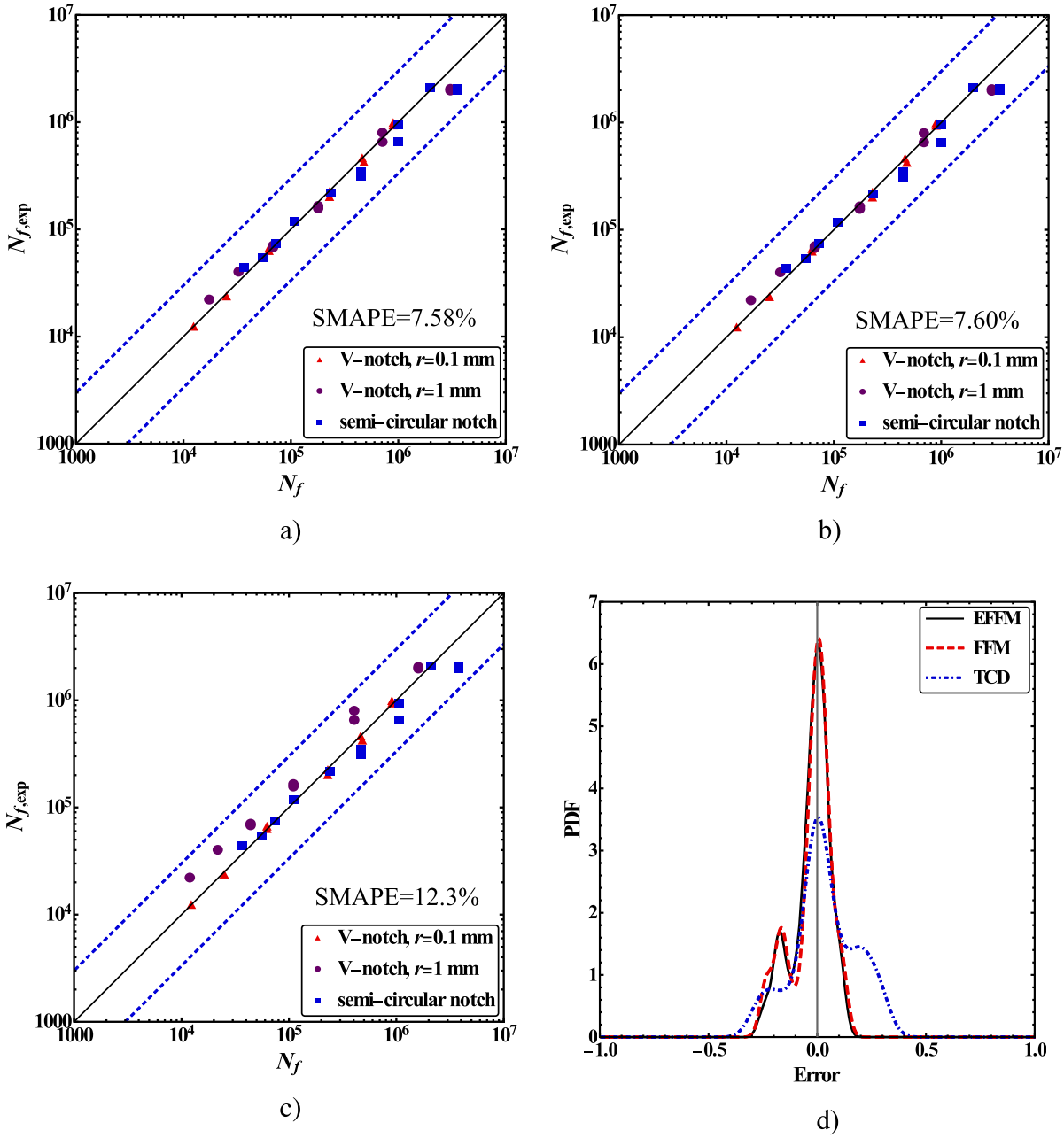

Fig. 5 Number of cycles to failure for different notch geometries and manufacturing angles made of Inconel 718 (R = 0): experimental data (Solberg and Berto 2019) vs. estimations by **a** EFFM, **b** FFM and **c** TCD methods. **d** Shows the PDF of the logarithmic error in the prediction of fatigue lifetime using EFFM, FFM, and TCD methods

Fig. 5 presents the predictions of fatigue life obtained employing EFFM, FFM and TCD methods, along with the corresponding experimental values. Additionally, it includes an analysis of the error PDF for further evaluation.

The results presented in Fig. 5 provide compelling evidence that both EFFM and FFM models outperform the TCD approach in predicting the fatigue life of specimens made of Inconel. Specifically, the lower SMAPE values achieved by the EFFM and FFM models (around 7.6% for both approaches) compared

to 12.3% for the TCD approach, indicate that the predicted fatigue life values are closer to the actual experimental values.

Figures 6 and 7 illustrate the experiments and the related theoretical predictions using the EFFM, FFM, and TCD models for the load ratios of 0.1 and − 1 for

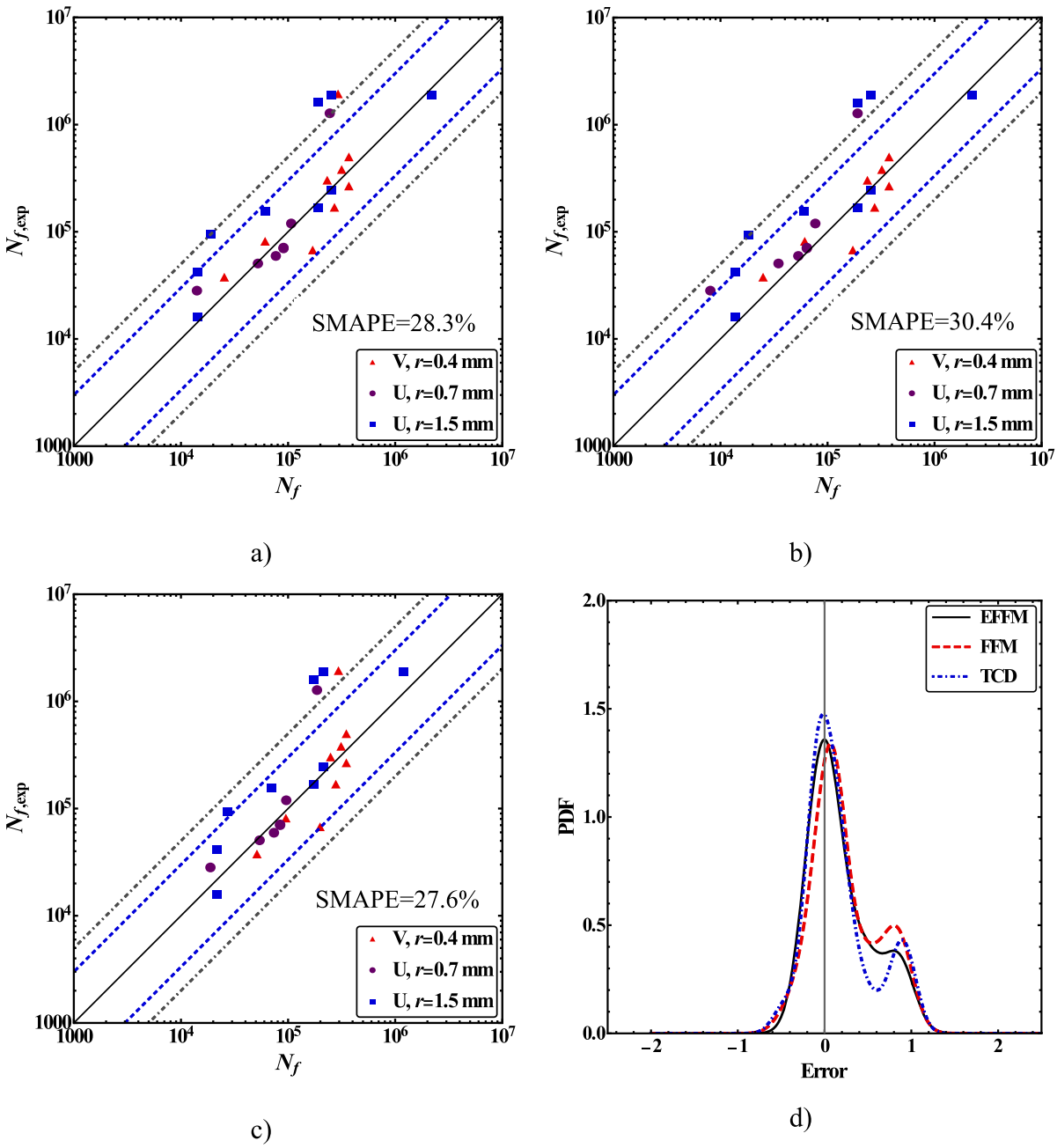

Fig. 6 Number of cycles to failure for different notch geometries and manufacturing angles made of Ti6Al4V under fatigue loading with loading ratio R = 0.1, experimental data (Zamzami et al. 2020) vs. estimations by **a** EFFM, **b** FFM and **c** TCD methods. **d** Shows the PDF of the logarithmic error in the prediction of fatigue lifetime using EFFM, FFM, and TCD methods

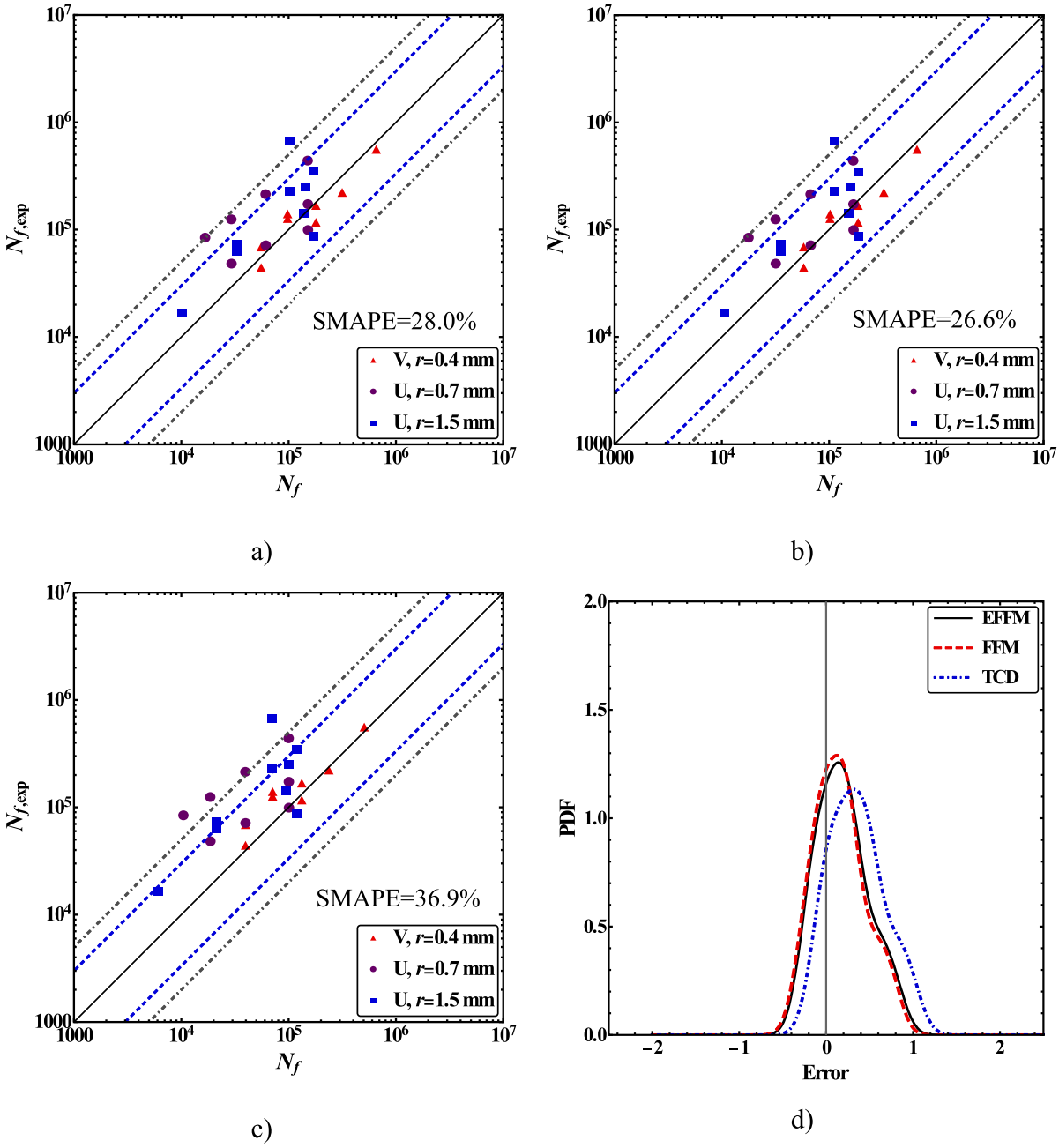

Fig. 7 Number of cycles to failure for different notch geometries and manufacturing angles made of Ti6Al4V under fatigue loading with loading ratio $R = -1$, experimental data (Zamzami et al. 2020) vs. estimations by **a** EFFM, **b** FFM and **c** TCD methods. **d** Shows the PDF of the logarithmic error in the prediction of fatigue lifetime using EFFM, FFM, and TCD methods

the specimens made of Ti6Al4V (Zamzami et al. 2020).

The fatigue life estimations for the Ti6Al4V alloy weakened by different notch geometries, as shown in Figs. 6 and 7, highlighted the overall stability and reliability of the proposed EFFM model. While the EFFM model did not consistently have the lowest SMAPE values across all conditions compared to the

FFM and TCD methods, it exhibited stable performance with relatively consistent predictive accuracy. This stability is crucial for ensuring reliable fatigue life predictions under the diverse loading scenarios presented here ($R = 0.1$ and $R = -1$). The PDFs of the logarithmic error further support this, indicating that EFFM maintains a balanced error distribution.

Besides the reasons mentioned in Sect. 2 for adopting a strain-based failure criterion, to further justify the more stable results of the proposed strain-based criterion compared to stress-based ones—specifically for the given set of experimental data—it can be noted that the layer-by-layer deposition in AM introduces microstructural anisotropy and defects (e.g., pores, lack of fusion, or residual stresses) that lead to localized strain concentrations. Furthermore, the anisotropic and heterogeneous nature of AM materials, influenced by build orientation and process parameters, makes strain-based approaches particularly effective in capturing direction-dependent damage evolution and failure patterns, especially for the first two datasets, where the material properties of different layers were averaged for use in the calculations. Finally, although the materials considered in this research were modeled as brittle, they are made of metal- or polymer-based materials and, based on the experimental load–displacement curve data, exhibited non-negligible extension beyond the elastic regime. It is worth mentioning that the aim of this research paper is not to showcase superior behavior but to compare the results with well-established criteria and provide a physically sound model. The focus is on proposing a fatigue criterion that is both valid and accurate, particularly in scenarios where strain is more reliable than stress, as discussed in Sect. 2. However, the proposed model generally performed the best among all three approaches. Further examination of other materials under diverse loading conditions, such as multiaxial loading, will help better assess the model's performance.

5 Conclusions

This paper proposes a new fatigue criterion called EFFM to assess the failure behavior of additive manufacturing materials. The model combines the non-local maximum normal strain criterion and Griffith energy balance, hence eliminating the need for empirical relationships to determine the critical distance and enabling the latter to account for crack initiation in a body without pre-existing cracks. The EFFM model predicts the fatigue life of any notch geometry using two material parameters that vary with the number of cycles according to power law equations. These parameters are cyclic strain and stress intensity factor at failure, which are obtained from strain-life data of plain and SIF-life of notched specimens.

To comprehensively evaluate the proposed model, five different sets of available experimental data involving various materials weakened by different notch geometries under diverse loading conditions were utilized. Using the SMAPE index and the PDF of logarithmic error, the EFFM model generally demonstrates greater accuracy and exhibits more stable performance than stress-based FFM and TCD in fatigue life estimation across various datasets for AM materials. It is worth emphasizing that the proposed approach can be used not only for AM samples but also for all other materials that fail under strain-controlled conditions.

Acknowledgements The authors acknowledge the funding from the European Union's Horizon 2020 research and innovation program under the Marie Skłodowska-Curie grant agreement No 861061—NEWFRAC Project.

Author contributions Conceptualization: [A.M.Mirzaei, A.H.Mirzaei]; Methodology: [A.M.Mirzaei, P. Cornetti]; Formal analysis and investigation: [A.M.Mirzaei, A.H.Mirzaei]; Software: [A.M.Mirzaei]; Writing—original draft preparation: [A.M.Mirzaei, A.H.Mirzaei]; Writing—review and editing: [P. Cornetti, A. Sapora]; Funding acquisition: [P. Cornetti]; Resources: [P. Cornetti]; Supervision: [P. Cornetti].

Funding This work was funded by HORIZON EUROPE Marie Sklodowska-Curie Actions, 861061.

Data availability No datasets were generated or analysed during the current study.

Declarations

Conflict of interest The authors declare no competing interests.

References

Aghabeigi M, Ayatollahi MR, Akbardoost J (2024) A new strain-based approach to investigate the size and geometry effects on fracture resistance of rocks. Theor Appl Fract Mech 134:104679. https://doi.org/10.1016/j.tafmec.2024.104679

Al Zamzami I, Razavi N, Berto F, Susmel L (2020) The critical distance method to estimate the fatigue strength of notched additively manufactured titanium alloys. Procedia Struct Integr 28:994–1001. https://doi.org/10.1016/j.prostr.2020.11.114

Ayatollahi MR, Torabi AR (2010) Brittle fracture in rounded-tip V-shaped notches. Mater des 31:60–67. https://doi.org/10.1016/j.matdes.2009.07.017

Basquin OH (1910) The exponential law of endurance tests. Proc Am Soc Test Mater 10:625–630

Benedetti M, Santus C (2019) Notch fatigue and crack growth resistance of Ti-6Al-4V ELI additively manufactured via selective laser melting: a critical distance approach to defect sensitivity. Int J Fatigue 121:281–292. https://doi.org/10.1016/j.ijfatigue.2018.12.020

Bidadi J, Aliha MRM, Akbardoost J (2022) Development of maximum tangential strain (MTSN) criterion for prediction of mixed-mode I/III brittle fracture. Int J Solids Struct 256:111979. https://doi.org/10.1016/j.ijsolstr.2022.111979

Blakey-Milner B, Gradl P, Snedden G et al (2021) Metal additive manufacturing in aerospace: a review. Mater des 209:110008

Branco R, Costa JD, Borrego LP et al (2021) Comparison of different one-parameter damage laws and local stress-strain approaches in multiaxial fatigue life assessment of notched components. Int J Fatigue 151:106405. https://doi.org/10.1016/j.ijfatigue.2021.106405

Burke-Veliz A, Syngellakis S, Reed PAS (2010) Fatigue crack shielding and deflection in plain bearings under large-scale yielding. Eng Fail Anal 17:648–657

Camanho PP, Erçin GH, Catalanotti G et al (2012) A finite fracture mechanics model for the prediction of the open-hole strength of composite laminates. Compos Part A Appl Sci Manuf 43:1219–1225. https://doi.org/10.1016/j.compositesa.2012.03.004

Campagnolo A, Berto F, Leguillon D (2016) Fracture assessment of sharp V-notched components under mode II loading: a comparison among some recent criteria. Theor Appl Fract Mech 85:217–226. https://doi.org/10.1016/j.tafmec.2016.02.001

Carpinteri A, Paggi M (2009) A unified interpretation of the power laws in fatigue and the analytical correlations between cyclic properties of engineering materials. Int J Fatigue 31:1524–1531. https://doi.org/10.1016/j.ijfatigue.2009.04.014

Carpinteri A, Cornetti P, Pugno N et al (2008) A finite fracture mechanics approach to structures with sharp V-notches. Eng Fract Mech 75:1736–1752. https://doi.org/10.1016/j.engfracmech.2007.04.010

Carpinteri A, Cornetti P, Pugno N (2009) Edge debonding in FRP strengthened beams: Stress versus energy failure criteria. Eng Struct 31:2436–2447. https://doi.org/10.1016/j.engstruct.2009.05.015

Carpinteri A, Cornetti P, Sapora A (2011) Brittle failures at rounded V-notches: a finite fracture mechanics approach. Int J Fract 172:1–8. https://doi.org/10.1007/s10704-011-9640-8

Castillo E, Fernández-Canteli A, Siegele D (2014) Obtaining S-N curves from crack growth curves: an alternative to self-similarity. Int J Fract 187:159–172. https://doi.org/10.1007/s10704-014-9928-6

Challamel N, Lanos C, Casandjian C (2005) Strain-based anisotropic damage modelling and unilateral effects. Int J Mech Sci 47:459–473. https://doi.org/10.1016/j.ijmecsci.2005.01.002

Chang KJ (1981) On the maximum strain criterion—a new approach to the angled crack problem. Eng Fract Mech 14:107–124

Ciavarella M, D'Antuono P, Demelio GP (2017) Generalized definition of "crack-like" notches to finite life and SN curve transition from "crack-like" to "blunt notch" behavior. Eng Fract Mech 179:154–164. https://doi.org/10.1016/j.engfracmech.2017.04.048

Cornetti P, Pugno N, Carpinteri A, Taylor D (2006) Finite fracture mechanics: a coupled stress and energy failure criterion. Eng Fract Mech 73:2021–2033. https://doi.org/10.1016/j.engfracmech.2006.03.010

Cornetti P, Sapora A, Carpinteri A (2013) Mode mixity and size effect in V-notched structures. Int J Solids Struct 50:1562–1582

Doitrand A, Cornetti P, Sapora A, Estevez R (2021) Experimental and theoretical characterization of mixed mode brittle failure from square holes. Int J Fract 228:33–43. https://doi.org/10.1007/s10704-020-00512-9

Dong XN, Luo Q, Sparkman DM et al (2010) Random field assessment of nanoscopic inhomogeneity of bone. Bone 47:1080–1084. https://doi.org/10.1016/j.bone.2010.08.021

Ezeh OH, Susmel L (2019) Fatigue strength of additively manufactured polylactide (PLA): effect of raster angle and non-zero mean stresses. Int J Fatigue 126:319–326. https://doi.org/10.1016/j.ijfatigue.2019.05.014

Ezeh OH, Susmel L (2020) On the notch fatigue strength of additively manufactured polylactide (PLA). Int J Fatigue 136:105583. https://doi.org/10.1016/j.ijfatigue.2020.105583

Gebhardt U, Gustmann T, Giebeler L et al (2022) Additively manufactured AlSi10Mg lattices – potential and limits of modelling as-designed structures. Mater des 220:110796. https://doi.org/10.1016/j.matdes.2022.110796

Ince A, Glinka G (2011) A modification of Morrow and Smith–Watson–Topper mean stress correction models. Fatigue Fract Eng Mater Struct 34:854–867

Jia Y, Bai Y (2016) Ductile fracture prediction for metal sheets using all-strain-based anisotropic eMMC model. Int J Mech Sci 115–116:516–531. https://doi.org/10.1016/j.ijmecsci.2016.07.022

Kholgh Eshkalak S, Rezvani Ghomi E, Dai Y et al (2020) The role of three-dimensional printing in healthcare and medicine. Mater des 194:108940. https://doi.org/10.1016/j.matdes.2020.108940

Leguillon D (2002) Strength or toughness? A criterion for crack onset at a notch. Eur J Mech 21:61–72

Lewandowski JJ, Seifi M (2016) Metal additive manufacturing: a review of mechanical properties. Annu Rev Mater Res 46:151–186

Marsavina L, Sapora A, Susmel L, Taylor D (2023) The application of the Theory of Critical Distances to nonhomogeneous materials. Fatigue Fract Eng Mater Struct 46:1314–1329. https://doi.org/10.1111/ffe.13922

Meyer G, Wang H, Mittelstedt C (2022) Influence of geometrical notches and form optimization on the mechanical properties of additively manufactured lattice structures. Mater des 222:111082. https://doi.org/10.1016/j.matdes.2022.111082

Miarka P, Seitl S, Bílek V, Cifuentes H (2022) Assessment of fatigue resistance of concrete: S-N curves to the Paris' law curves. Constr Build Mater 341:127811. https://doi.org/10.1016/j.conbuildmat.2022.127811

Mirone G (2004) Approximate model of the necking behaviour and application to the void growth prediction. Int J Damage Mech 13:241–261. https://doi.org/10.1177/1056789504042592

Mirsayar MM (2015) Mixed mode fracture analysis using extended maximum tangential strain criterion. Mater des 86:941–947

Mirsayar MM (2022) Maximum principal strain criterion for fracture in orthotropic composites under combined tensile/shear loading. Theor Appl Fract Mech 118:103291. https://doi.org/10.1016/j.tafmec.2022.103291

Mirsayar MM, Razmi A, Aliha MRM, Berto F (2018) EMTSN criterion for evaluating mixed mode I/II crack propagation in rock materials. Eng Fract Mech 190:186–197

Mirzaei AM (2024) Stress, strain, or energy? Which one is superior predictor of fatigue life in notched Components? A novel machine learning-based framework. Eng Fract Mech 309:110401. https://doi.org/10.1016/j.engfracmech.2024.110401

Mirzaei AH, Shokrieh MM (2024) Progressive fatigue damage modeling of laminated composites using strain-based failure criteria. J Compos Mater 58:519–531. https://doi.org/10.1177/00219983241227098

Mirzaei AM, Ayatollahi MR, Bahrami B (2019) Asymptotic stress field and the coefficients of singular and higher order terms for V-notches with end holes under mixed-mode loading. Int J Solids Struct. https://doi.org/10.1016/j.ijsolstr.2019.05.011

Mirzaei AM, Ayatollahi MR, Bahrami B, Berto F (2020) Elastic stress analysis of blunt V-notches under mixed mode loading by considering higher order terms. Appl Math Model 78:665–684. https://doi.org/10.1016/j.apm.2019.09.049

Mirzaei AM, Ayatollahi MR, Bahrami B, Berto F (2021a) A new unified asymptotic stress field solution for blunt and sharp notches subjected to mixed mode loading. Int J Mech Sci 193:106176. https://doi.org/10.1016/j.ijmecsci.2020.106176

Mirzaei AM, Corrado M, Sapora A, Cornetti P (2021b) Analytical modeling of debonding mechanism for long and short bond lengths in direct shear tests accounting for residual strength. Materials (Basel). https://doi.org/10.3390/ma14216690

Mirzaei AM, Cornetti P, Sapora A (2023) A novel finite fracture mechanics approach to assess the lifetime of notched components. Int J Fatigue. https://doi.org/10.1016/j.ijfatigue.2023.107659

Molaei R, Fatemi A (2021) Fatigue performance of additive manufactured metals under variable amplitude service loading conditions including multiaxial stresses and notch effects: experiments and modelling. Int J Fatigue 145:106002. https://doi.org/10.1016/j.ijfatigue.2020.106002

Molaei R, Fatemi A, Phan N (2022) Notched fatigue of additive manufactured metals under axial and multiaxial loadings, part II: data correlations and life estimations. Int J Fatigue 156:106648. https://doi.org/10.1016/j.ijfatigue.2021.106648

Nalla RK, Kinney JH, Ritchie RO (2003) Mechanistic fracture criteria for the failure of human cortical bone. Nat Mater 2:164–168

Priel E, Yosibash Z, Leguillon D (2008) Failure initiation at a blunt V-notch tip under mixed mode loading. Int J Fract 149:143–173

Rosendahl PL, Staudt Y, Schneider AP et al (2019) Nonlinear elastic finite fracture mechanics: modeling mixed-mode crack nucleation in structural glazing silicone sealants. Mater des 182:108057. https://doi.org/10.1016/j.matdes.2019.108057

Salvati E, Lunt AJG, Heason CP et al (2020) An analysis of fatigue failure mechanisms in an additively manufactured and shot peened IN 718 nickel superalloy. Mater des 191:108605. https://doi.org/10.1016/j.matdes.2020.108605

Sanaei N, Fatemi A (2020) Analysis of the effect of internal defects on fatigue performance of additive manufactured metals. Mater Sci Eng A 785:139385. https://doi.org/10.1016/j.msea.2020.139385

Sapora A, Cornetti P, Carpinteri A (2014) V-notched elements under mode II loading conditions. Struct Eng Mech 49:499–508

Schmidt J, O'Neill M, Dirks J-H, Taylor D (2020) An investigation of crack propagation in an insect wing using the Theory of Critical Distances. Eng Fract Mech 232:107052. https://doi.org/10.1016/j.engfracmech.2020.107052

Shi L, Kang J, Gesing M et al (2020) Fatigue life assessment of Al-steel resistance spot welds using the maximum principal strain approach considering material inhomogeneity. Int J Fatigue 140:105851. https://doi.org/10.1016/j.ijfatigue.2020.105851

Solberg K, Berto F (2019) Notch-defect interaction in additively manufactured Inconel 718. Int J Fatigue 122:35–45. https://doi.org/10.1016/j.ijfatigue.2018.12.021

Song X, Feih S, Zhai W et al (2020) Advances in additive manufacturing process simulation: residual stresses and distortion predictions in complex metallic components. Mater des 193:108779. https://doi.org/10.1016/j.matdes.2020.108779

Susmel L (2009) Multiaxial notch fatigue. Woodhead Publishing, Oxford

Susmel L, Taylor D (2007) A novel formulation of the Theory of Critical Distances to estimate lifetime of notched components in the medium-cycle fatigue regime. Fatigue Fract Eng Mater Struct 30:567–581

Susmel L, Taylor D (2008a) The Theory of Critical Distances to predict static strength of notched brittle components subjected to mixed-mode loading. Eng Fract Mech 75:534–550. https://doi.org/10.1016/J.ENGFRACMECH.2007.03.035

Susmel L, Taylor D (2008b) On the use of the Theory of Critical Distances to predict static failures in ductile metallic materials containing different geometrical features. Eng Fract Mech 75:4410–4421. https://doi.org/10.1016/j.engfracmech.2008.04.018

Susmel L, Taylor D (2008c) The modified Wöhler curve method applied along with the Theory of Critical Distances to estimate finite life of notched components subjected to complex multiaxial loading paths. Fatigue Fract Eng Mater Struct 31:1047–1064. https://doi.org/10.1111/j.1460-2695.2008.01296.x

Susmel L, Taylor D (2010) An elasto-plastic reformulation of the theory of critical distances to estimate lifetime of notched components failing in the low/medium-cycle fatigue regime. J Eng Mater Technol. https://doi.org/10.1115/1.4000667

Susmel L, Taylor D (2011) The Theory of Critical Distances to estimate lifetime of notched components subjected to variable amplitude uniaxial fatigue loading. Int J Fatigue 33:900–911. https://doi.org/10.1016/j.ijfatigue.2011.01.012

Susmel L, Taylor D (2013) The Theory of Critical Distances to estimate finite lifetime of notched components subjected to constant and variable amplitude torsional loading. Eng Fract Mech 98:64–79. https://doi.org/10.1016/j.engfracmech.2012.12.007

Susmel L, Taylor D (2015) Estimating lifetime of notched components subjected to variable amplitude fatigue loading according to the elastoplastic Theory of Critical Distances. J Eng Mater Technol. https://doi.org/10.1115/1.4028927

Taylor D (1999) Geometrical effects in fatigue: a unifying theoretical model. Int J Fatigue 21:413–420. https://doi.org/10.1016/S0142-1123(99)00007-9

Taylor D, Bologna P, Bel Knani K (2000) Prediction of fatigue failure location on a component using a critical distance method. Int J Fatigue 22:735–742. https://doi.org/10.1016/S0142-1123(00)00062-1

Timoshenko S (1983) History of strength of materials: with a brief account of the history of theory of elasticity and theory of structures. Courier Corporation

Wang Y, Sun C, Ghadimi S et al (2023) StrainNet: improved myocardial strain analysis of cine MRI by deep learning from DENSE. Radiol Cardiothorac Imaging 5:e220196. https://doi.org/10.1148/ryct.220196

Whitney JM, Nuismer RJ (1974) Stress fracture criteria for laminated composites containing stress concentrations. J Compos Mater 8:253–265

Wu J-Y, Cervera M (2016) A thermodynamically consistent plastic-damage framework for localized failure in quasi-brittle solids: material model and strain localization analysis. Int J Solids Struct 88–89:227–247. https://doi.org/10.1016/j.ijsolstr.2016.03.005

Yosibash Z, Priel E, Leguillon D (2006) A failure criterion for brittle elastic materials under mixed-mode loading. Int J Fract 141:291–312

Zhao J, Tang J, Wu HC (1998) A reliability assessment method in strain-based fatigue life analysis. J Press Vessel Technol 120:99–104. https://doi.org/10.1115/1.2841893

Zhu S-P, Lei Q, Huang H-Z et al (2017) Mean stress effect correction in strain energy-based fatigue life prediction of metals. Int J Damage Mech 26:1219–1241. https://doi.org/10.1177/1056789516651920

Zhu S-P, He J-C, Liao D et al (2020) The effect of notch size on critical distance and fatigue life predictions. Mater des 196:109095. https://doi.org/10.1016/j.matdes.2020.109095

Zhu F, Liu H, Yao L, Mei G (2021) Study on the maximum tangential strain criterion for the initiation of the wing-crack under uniaxial compression. Theor Appl Fract Mech 116:103085. https://doi.org/10.1016/j.tafmec.2021.103085

Zywicz E (1999) On the equivalence of stress- and strain-based failure criteria in elastic media. Eur J Mech - A/Solids 18:391–398. https://doi.org/10.1016/S0997-7538(99)00129-1